International Journal of Mechanical Engineering
ISSN : 2277-7059 Volume 2 Issue 5 (May 2012)
http://www.ijmejournal.com/ https://sites.google.com/site/journalijme/

EFFECTS OF INERTIA AND PROCESS PARAMETERS ON ISOTHERMAL HIGH SPEED TWO-LAYER FILAMENT JET FLOW

Md. Abdul Wakil, Z. U. Ahmed
Department of Mechanical Engineering, Khulna University of Engineering & Technology, Khulna-9203, Bangladesh

Abstract: This paper investigates the influences of inertia and process parameters on two-layer fiber spinning process for incompressible, isothermal and Newtonian filament jet flow. The present study focuses on the steady flow considering inertia, gravity and non-uniform velocity of each layer across the fiber. The governing equations are solved numerically as nonlinear two-point boundary value problem given the analytical solution is practically impossible. The effects of inertia and initial process conditions (draw ratio, initial velocity ratio and die exit radius ratio) are discussed. The velocity increases monotonically with the axial position in each layer due to inertia effect, at a rate that is relatively slower (faster) near the spinneret (take-up point) as Re increases. In contrast, the radii decrease monotonically with the axial position in each layer.

.**Keywords:** Fiber spinning, Draw ratio, Boundary value problem.

1. Introduction

In a typical fiber spinning process, a thin cylinder is manufactured by extruding the molten polymer through a spinneret. The molten fiber is normally stretched in length and drawn to reduce its diameter. With appropriate draw ratio (ratio of the take-up velocity to the extrusion velocity at the spinneret) the desired fiber diameter can be obtained. In the actual process, a bundle of many filaments are extruded and stretched together [1], hence, it is important to investigate multilayer fiber spinning process. The fiber with multi-layer filament jets has constantly been enlarged in various applications, for example, in plastic fabrication process, inserting batteries, placing colors, burying recycled materials, coatings for controlling film surface properties etc [2]. One of the major instability and defects which limits the productivity in industrial operation is draw resonance. The draw resonance appears typically at high draw ratios. There exists a critical draw ratio, beyond which stable operation is impossible and draw resonance instability is observed.

Extensive studies have been conducted on fiber spinning of Newtonian and non-Newtonian fluid since early 1960’s when draw resonance was first introduced by Christensen [3] and Miller [4]. The previous experimental and theoretical studies on the fiber spinning process are mostly focused on single-layer flow [see, for instances 5-10], and most of the studies were without inertia, gravity, and surface tension. The inertia and gravity can, however, play an important role in stability of the real process, which is shown by Shah and Pearson [11] in their stability analysis. The effects of inertia on fiber spinning process, which have not been investigated in detail, especially about their compound effect, is one of the main objective in the present study.

Although significant studies, either theoretical or experimental, are available for single-layer fiber spinning, the investigation on multilayer fiber spinning, even on film casting, is very limited in literature. Park [12] performed the first theoretical analysis on two-layer film casting, where one layer was Newtonian and another was Upper-Convected Maxwell fluid. Using simple constitutive models, he investigated the effects of the interaction between two fluids with different rheological properties on the film thickness and stress profiles. Co et al. [13, 14] adopted a similar assumption and studied the multi-layer film casting of modified Giesekus fluids. Recently, the film casting of multi-layer flows of Newtonian fluid and non-Newtonian fluid was studied by Zhang et al. [15] and Lee et al. [16], respectively. Of closer relevance to the present study is the investigation of Suman and Tandon [17] who examined the three-layer flow stability of fiber drawing for both Newtonian and non-Newtonian fluids of constant densities in the absence of inertia, gravity and surface tension. They derived the governing equations as slender jet approximation, and did not treat three layers separately. They, instead, used a combined momentum balance equation. They imposed continuity of velocity vector on the layer interface, which predicts uniform velocities across the fiber cross section regardless the shearing in the layers. This prediction of continuous velocity at the interface was reported somewhat erroneous by Zhang et al. [15], who reported that there is bound to be a certain amount of shearing that increases with the viscosity ratio, hence the axial velocity cannot be (even approximately) uniform across the entire film. For the case of isothermal Newtonian drawing, Suman and Tandon [17] predicted the critical draw ratio for multi-layered fiber is 20.21, which is the same value that has been reported for the single layer fiber spinning.

The major objective of this study is to investigate how the kinematics of the two-layer fiber spinning flow is affected in the presence of inertia and gravity when non-uniform velocity of each layer across the fiber is considered. The numerical results predicts the influence of inertia and other process parameters, such as the draw ratio, the initial velocity ratio and the die-exit radius ratio on the steady state flow will be investigated. It can be noted that the influence of gravity and other rheological properties like density ratio and viscosity ratio of the two layers were discussed elsewhere by the same authors [18], thus their influence on the flow will not be repeated here.

2. Problem formulation

Consider an axisymmetric, two-layer incompressible, Newtonian and isothermal fiber exiting from spinneret is drawn continuously and wrapped by the rotating cold roll at some distance down from the spinneret. The distance between the spinneret and the chill roll is L. The jet is assumed to exit from two concentric circular tube type die, where one layer exits from the inner circular tube and the other layer, which completely surrounds the inner layer, exits from the thin annulus in between the circular tubes. The two layers, inner layer (layer 1) and outer layer (layer 2), are assumed immiscible, and attach each other immediately after the spinneret. The problem is schematically described in figure 1. The radii of inner and outer layer are R^1 and R^2, respectively. The densities and viscosities of layer 1 and layer 2 are ρ^1 and ρ^2, and viscosities μ^1 and μ^2, respectively. The problem is formulated in the (r, θ, X) space with r, θ and X axis coinciding with the radial, azimuthal and axial directions. The corresponding velocities in the axis directions are (U_r, U_θ, U_x). The radii of two-layer fiber and mean velocities at the spinneret (X =

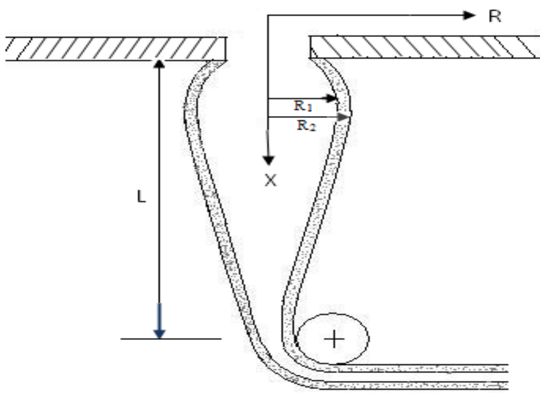

Figure 1. Schematic illustration of the two-layer fiber spinning process

0) are, R_0^1 and R_0^2 and U_{x0}^1 and U_{x0}^2. The fiber drawing length (air gap) between the spinneret and winder/chill roll is L. The die swell is also ignored, considering the variation of fiber radius is small. The flow is assumed to be dominant axial velocity that is uniform across each layer separately indicating the flow is predominantly elongational. The stream wise velocities of two layers are, thus,

functions of axial direction X and time t only. Under these assumptions and in the presence of inertia and gravity force, the conservations of mass and momentum reduce, respectively, to

$$\frac{1}{r}\frac{\partial}{\partial r}\left(rU_r^i\right)+\frac{\partial U_X^i}{\partial X}=0, \tag{1}$$

$$\rho^i\left(U_{X,\tau}^i+U_X^iU_{X,X}^i\right)=\sigma_{XX,X}^i+\frac{1}{r}\left(r\sigma_{rX}^i\right)_{,r}+\rho^i g, \tag{2}$$

where i refers to 1 or 2 for layer 1 or layer 2, respectively, and a subscript after a comma denote a partial differentiation. Here σ_{XX} and σ_{rX} are the normal and shear stress, respectively, g is the gravitational acceleration, and τ is the time.

The interfacial condition for multi-layer fluid flow is different from the single layer flow where no traction at the interface is considered. Suman and Tandon [17], in their study on multi-layer fiber drawing, applied no-slip boundary condition at the interface of two fluids result in the constant axial velocity across the whole cross section of fiber regardless of the viscosity ratio of the two layers. Zhang et al. [15], however, reported that the boundary conditions at the interface between two layers, namely the continuity of the axial velocity i.e. no-slip condition and the traction, cannot be simultaneously accommodated. Thus either the velocity or the traction can be continuous across the interface. However, in addition to the constant axial velocity across the fiber, the imposition of continuity of velocity across the interface is neglected for two other reasons, as reported by Zhang et al. [15] in their two-layer film casting process. Firstly, in the real two-layer process, a certain amount of shearing increases with the viscosity ratio indicating the axial velocity cannot be (even approximately) uniform across the entire film. In fact, in the limit of zero or infinite viscosity ratio, one of the layers is effectively a solid, resulting in the formation of a boundary layer. Secondly, there exists a possibility of considerable slip at the interface, for instance, the case where the fluid in contact with the chill roll is the less viscous layer. Since the flow in this layer is predominantly elongational, it may fail to fully entrain the second layer, resulting in slip. Thus, following Zhang et al. [15], in the present study, the continuity of traction is ensured at the interface, and the axial velocity is assumed to be uniform across each fiber layer separately. Therefore, the boundary conditions for system of governing equations (1) and (2) are prescribed as follows.

At the spinneret (X = 0) and the chill roll (X = 1), the velocities in the axial direction are given as

$$U_X^1(X=0,\tau)=U_{X0}^1,\quad U_X^2\ (X=0,\tau)=U_{X0}^2,\quad U_X^1(X=L,\tau)=U_{XL}^1 \tag{3}$$

The fiber radius of each layer at X = 0 is given as

$$R^1(X=0,\tau)=R_0^1,\quad R^2(X=0,\tau)=R_0^2, \tag{4}$$

where R^1 and R^2 are the fiber radius of layer 1 and layer 2, respectively. The traction of the two layers, $\mathbf{t}^1$ and $\mathbf{t}^2$, are continuous at the interface:

$$\mathbf{t}^1\left(r=R^{1-},\tau\right)=\mathbf{t}^2\left(r=R^{1+},\tau\right), \tag{5}$$

where R^{1-} and R^{1+} denote the interfacial radii for the layer 1 and layer 2, respectively.

Noting that the molten polymer has a high viscosity and the fiber radius varies slowly, surface tension and air drag are assumes to be negligible, leading to the following dynamic condition of the free surfaces:

$$\mathbf{t}^2\left(r=R^2,\tau\right)=0. \tag{6}$$

Upon using the boundary conditions, the following non-dimensional governing equations are obtained,

$$\delta^{1^2},_t+\left(\delta^{1^2}U_x^1\right),_x=0, \tag{7}$$

$$\delta^{o^2},_t+\left(\delta^{o^2}U_x^2\right),_x=0 \tag{8}$$

$$\frac{Re}{3}\begin{bmatrix}\left(\delta^{1^2}+R_\rho R_\mu \delta^{o^2}\right)u^1_{x,t}+\left(\delta^{1^2}+R_\rho R_\mu^2 \delta^{o^2}\right)u^1_x u^1_{x,x} \\ +R_\rho R_\mu \delta^{o^2}\left(R_U-R_\mu\right)u^1_{x,x}\end{bmatrix}=\left[\left(\delta^{1^2}+\delta^{o^2}\right)u^1_{x,x}\right]_{,x}+\frac{Re}{3Fr}\left(\delta^{1^2}+R_\rho \delta^{o^2}\right), \quad (9)$$

$$u^2_x = R_\mu\left(u^1_x-1\right)+R_U, \quad (10)$$

where $\delta^{o^2}=\delta^{2^2}-\delta^{1^2}$ in equations (15) and (16). The boundary conditions are reduced to

$$u^1_x(x=0,t)=1, \quad u^1_x(x=1,t)=Dr, \quad \delta^1(x=0,t)=1, \quad \delta^2(x=0,t)=R_r. \quad (11)$$

The details of the derivation for the equations (7-11) are obtained in the reference [18]. In this case, L is taken as the reference length, U^1_{x0} the reference velocity, and R^1_0 the reference radius. The dimensionless variables evolved in the equations are defined as follows

$$x=\frac{X}{L}, \quad t=\frac{U^1_{x0}\tau}{L}, \quad u^i_x=\frac{U^i_x}{U^1_{x0}}, \quad \delta^i=\frac{R^i}{R^1_0}, \quad (12)$$

and six non-dimensional parameters emerge in the problem, namely the draw ratio, Dr, the velocity ratio, R_U, the density ratio, R_ρ, the viscosity ratio, R_μ, the Froude number, Fr, as well as Reynolds number, Re, are introduced as

$$Dr=\frac{U^1_{xL}}{U^1_{x0}}, \quad R_r=\frac{R^2_0}{R^1_0}, \quad R_U=\frac{U^2_{x0}}{U^1_{x0}}, \quad R_\rho=\frac{\rho^2}{\rho^1}, \quad R_\mu=\frac{\mu^1}{\mu^2}, \quad Fr=\frac{U^{1^2}_{x0}}{gL}, \quad Re=\frac{\rho^1 U^1_{x0} L}{\mu^1}. \quad (13)$$

One can readily be solved the steady state radii in terms of velocities as follows

$$\delta^{1s}=\frac{1}{\sqrt{u^{1s}_x}}, \qquad \delta^{os}=\sqrt{\frac{R_r{}^2 R_U}{R_\mu\left(u^{1s}_x-1\right)+R_U}}, \quad (14)$$

and upon substituting these expressions and the steady state velocity of layer 2 (Eq. 10) into (9), the equation for the velocity of layer 1 is obtained,

$$\frac{Re}{3}\begin{bmatrix}\left(\delta^{1s^2}+R_\rho R_\mu^2 \delta^{os^2}\right)u^{1s}_x u^{1s}_{x,x} \\ +R_\rho R_\mu \delta^{os^2}\left(R_U-R_\mu\right)u^{1s}_{x,x}\end{bmatrix}=\left[\left(\delta^{1s^2}+\delta^{os^2}\right)u^1_{x,x}\right]_{,x}+\frac{Re}{3Fr}\left(\delta^{1s^2}+R_\rho \delta^{os^2}\right), \quad (15)$$

with the boundary conditions

$$u^{1s}_x(x=0)=1, \qquad u^{1s}_x(x=1)=Dr. \quad (16)$$

Due to the unavailability of analytical solution, the equation (15) with conditions (16) is solved numerically by two-point boundary value problem using MATLAB. The coupled governing equation is recast as the system of first order equation. The nonlinear system is solved by using function 'bvp4c'. Numerical solution is obtained by solving a global system of algebraic equations stemming from the boundary conditions. The mesh is chosen adaptively to make the local error in the tolerance limit, which is chosen 1e-6 for all computations.

3. Discussion and results:

In this section, the results of the numerical solution are presented for the two-layer fiber spinning flow systematically for the effects of inertia, the draw ratio the velocity ratio and the radius ratio. The velocity profiles and the fiber radii distributions for each layer are determined.

3.1 Effect of inertia: The influence of inertia on the two-layer fiber spinning flow is examined in figure 2 by varying the Reynolds number over the range $Re \in [0,2]$ for $D_r = 15$, $R\mu = 1.5$, $R\rho = 0.5$, $Fr = 1$. The ratio of initial fiber radii R_r and the reference velocity ratio, R_u at the spinneret is taken as

1.2 and 1, respectively. In order to dominate the influence of inertia over the effect of gravity, since the effects are opposite in single layer, the gravitational effect is chosen sufficiently small (Fr =1). The flow responses are depicted in figure 2a-2d, where the velocity and fiber radius for layer 1, $u^{(1)s}(x)$ and $\delta^{(1)s}(x)$, are shown in figure 2a and 2b, respectively, and for layer 2, $u^{(2)s}(x)$ and $\delta^{(2)s}(x)$, in figure 2c and 2d, respectively. The results show that the velocity increases monotonically with x in each layer, at a rate that is relatively slower (faster) near the spinneret (take-up point) as Re increases. The velocity in layer 2 at the take-up is larger than that of layer 1, despite the equal velocity imposed at the spinneret. This is particularly due to the response of the viscosity ratio. For the equal reference velocity ratio and viscosity ratio the velocity of layer 2 will be larger or smaller than the velocity of layer 1 by a factor equal to viscosity ratio (see the relation 10). Interestingly, the velocity of each layer at the take-up merge to a point, and thus independent of inertia. This observation is of course expected for layer 1 to

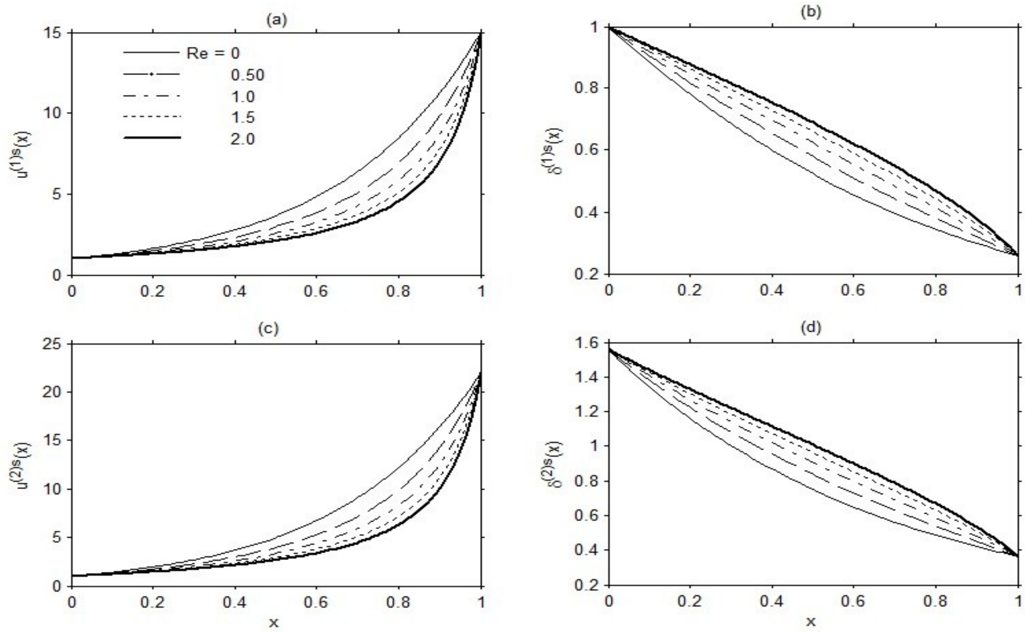

Figure2. Influence of inertia on the velocity and radius in layer 1 (a,b) and layer 2 (c,d) $Re \in [0,2], R_\rho = 0.5, R_\mu = 1.5, R_r = 1.2, R_u = Fr = 1, D_r = 15.$

satisfy the boundary condition (11), while it is less obvious regarding layer 2. This is, however, confirmed from the relation (10), which shows that $u_x^{(2)} = R_\mu\left(u_x^{(1)} - 1\right) + R_u$ is indeed independent of Re. The radii decrease monotonically with x in each layer. Both the layers have similar qualitative behavior with Re. The decreasing tendency is almost linear for Re close to unity, however, the decreasing rate is faster near the spinneret and close to the take-up region for smaller inertia values (Re less than unity) and higher inertia values (Re greater than unity), respectively (see figures 2b and 2d).

The overall velocity and radius deviates from the exponential behavior as inertia increases, reflecting an augmentation of the nonlinear character of the flow. It can be annotated that the velocity profile and the film fiber radius distribution along the x direction coincide with those of the single-layer fiber flow [19], if the flow parameters in the two-layer problem are chose such that Rμ =Rρ =Ru =1.

3.2 Influence of draw ratio: The effect of draw ratio is thus examined in figure 3 for the velocity (3a, 3c) and radius (3b, 3d) profile in each layer in the Dr range from 5 to 25. The other parameters are R_μ= 1.5, R_ρ= 0.5, R_r= 1.2, Re = 1, Fr = 1 and R_u = 1. Overall, the fiber radii and the velocity distributions are sensitive to Dr, but the influence of the draw ratio is strongest near the take-up point. The velocity increases with draw ratio, and the rate of increase of velocity at the take-up seems linear in the given draw ratio range (see figure 3a and 3c), whereas the change of velocity tends to insignificant when approaching to the spinneret.

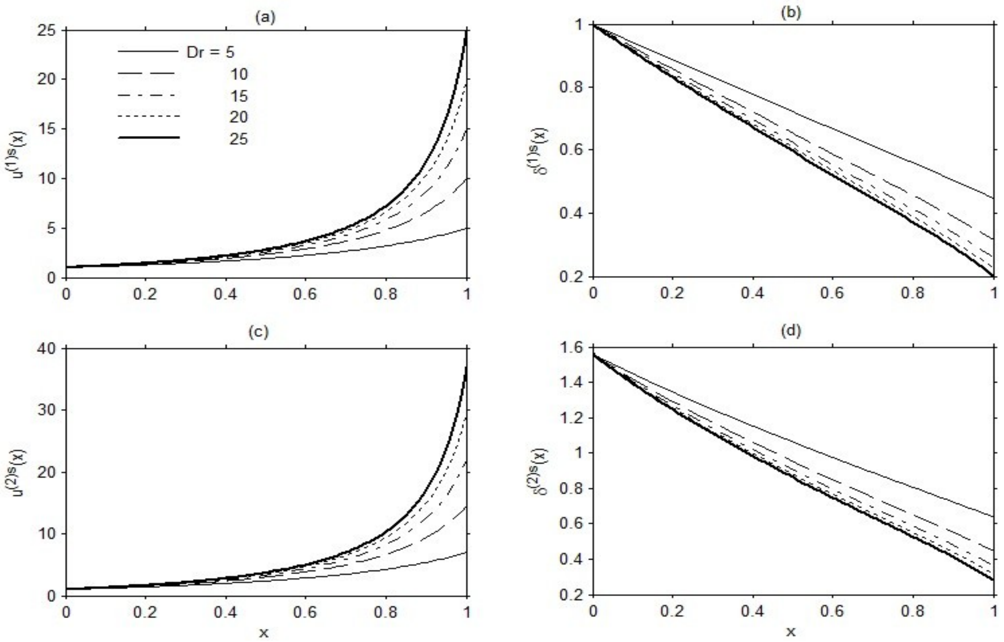

Figure3. Influence of draw ratio on the velocity and radius of layer 1 (a, b) and layer 2 (c, d) for $Dr \in [5,25]$, $R_\rho = 0.5$, $R_\mu = 1.5$, $R_r = 1.2$, $R_u = Fr = 1$, $R_e = 1$.

The velocities at the take-up point in layer 1 and layer 2 follows from the boundary condition and equation (9), respectively, and can be written as $u^{(1)s}(x=1) = Dr$ and $u^{(2)s}(x=1) = 1.5Dr - 0.5$. On the other hand, the film radii decreases linearly with the position for all draw ratios. The film radius at the take-up point decreases with the increase of draw ratios in both layers, however, more significantly in layer 1. For large draw ratios, the radii seem to have insignificant change with Dr (see figures 3b and 3d). The radii at the take-up point are given as $1/\sqrt{Dr}$ in layer 1, and $1/\sqrt{1.5\,Dr - 0.5}$ in layer 2.

3.3 Influence of reference velocity ratio: The influence of the reference velocity ratio (the ratio of velocities at the spinneret at layer 2 and layer 1) on the fiber spinning flow is discussed in figure 4 over the velocity ratio range $R_u \in [0.5, 1.5]$, where figures 4a and 4b, and 4c and 4d show the velocity and radius profiles of layer 1 and layer 2, respectively The remaining parameters are fixed at, $Re = 1$ $R_\rho = 0.5$, $R_\mu = 1.5$, $R_r = 1.2$, $Fr = 1$ and Dr = 15. The results show that the velocity (thickness) of two layers increases (decreases) monotonically against the spinning distance, similarly to the figures 2a and 2c. However, the velocity of layer 1 is almost independent of velocity ratio, whereas the velocity of layer 2 increases moderately with R_u, particularly close to the spinneret. This observation is attributed to the limitations of layer 1 by boundary conditions at the spinneret and take-up. Similarly to the effect of inertia, nonlinear character of the flow is observed at close to the take-up region whatever the velocity ratio is imposed at the spinneret. The change of velocity in layer 2 with R_u is insignificant near the take-up where this comparatively small change in velocity is overlooked by the draw ratio. The thickness profiles deviate from nonlinear behavior to linear profile for the whole spinning distance, which is particularly true for layer 1 and for layer 2 with R_u equal to or lager than unity. R_u has no influence on the fiber radius of layer 2 at the die exit region, which, however, has significant influence at the take up point and fiber radius increases with the increase of R_u.

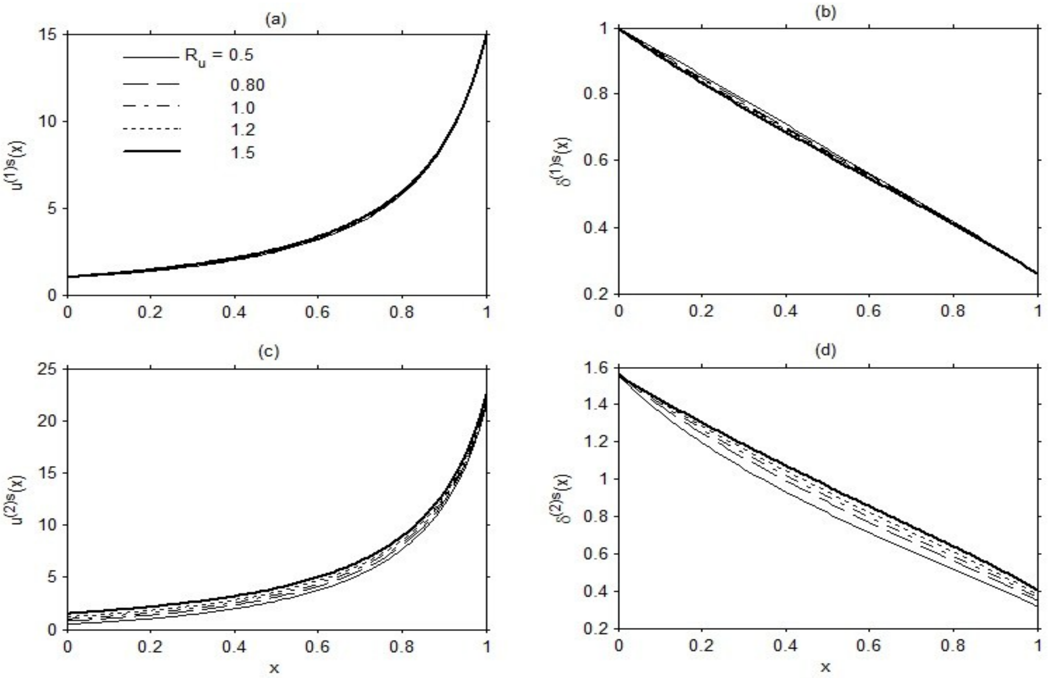

Figure4. Influence of initial velocity ratio on the velocity and radius for $R_u \in [0.5, 1.5]$, $R_\rho = 0.5, R_\mu = 1.5, R_r = 1.2, Fr = 1, R_e = 1, D_R = 15$

3.4 Effect of reference radius ratio: The two-layer fiber typically obtains from two concentric circular die exits. The influence of die exit for single layer flow is not obvious, thus never investigated. However, for multiple layer flow this process condition may have some influence, which will be seen next.If the outer die exit sets far away from the inner die exit, the two layers essentially will be separate, and will flow through the spinning distance separately. The two-layer flow will not be obvious in this case. Thus, the effect of reference radius ratio (same as die radius ratio) is shown in figure 5 by varying R_r while keeping other parameters fixed. The radius ratio varies from 1 to 2 and other parameters are taken as $R_\rho = 0.5, R_\mu = 1.5, R_u = 1, Fr = 1, R_e = 1, D_R = 15$.It is evident from figures that R_r has no influence on the layer 1 and the velocity of layer 2. However, fiber radius in layer 2 is significantly influenced by R_r. The decreasing linear distributions of radius again are observed with the position x. The neck-in tendency of fiber radius is more with the increase of R_r near the take-up region.

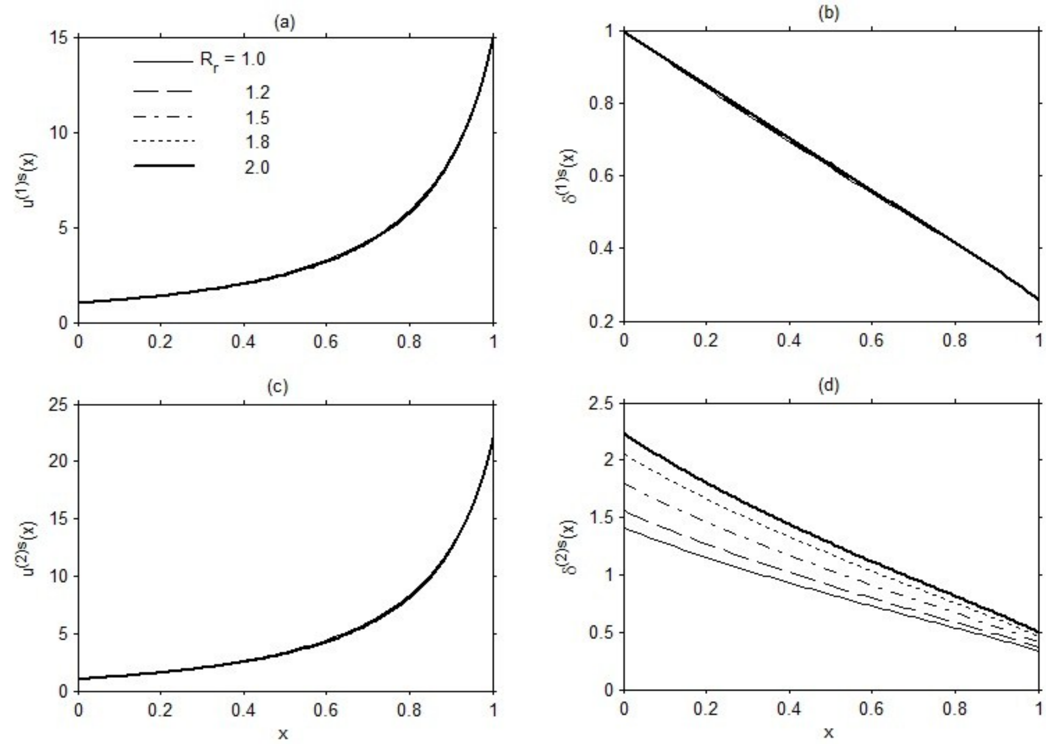

Figure5. Influence of the reference radius ratio on velocity and radius of layer 1 (a, b) and layer 2 (c, d) for $R_r \in [1,2], R_\rho = 0.5, R_\mu = 1.5, R_u = 1, Fr = 1, R_e = 1, D_R = 15$

4 Conclusions:

In this study, the steady, incompressible two-layer fiber spinning process is investigated. Due to the unavailability of analytical solution, the governing equations are solved numerically by two-point nonlinear boundary value problem. The effect of inertia and process parameters such as the draw ratio, the initial velocity ratio and the die radius ratio, on the velocity and fiber radius distributions for each layer is examined for a wide range of parameters. The results are summarized below.

The velocity and radius increases monotonically with the position in each layer. For the equal initial velocity ratio and viscosity ratio the velocity of layer 2 will be larger or smaller than the velocity of layer 1 by a factor equal to viscosity ratio. The decreasing tendency of radii is faster near the spinneret and close to the take-up region for smaller inertia values and higher inertia values, respectively.

Overall, the fiber radii and the velocity distributions are sensitive to draw ratio. The velocity increases with draw ratio, and the rate of increase of velocity at the take-up seems linear in the given draw ratio range. The film radius at the take-up point decreases more significantly in layer 1 with the increase of draw ratios. The velocity of layer 1 is almost independent of velocity ratio, whereas the velocity of layer 2 increases moderately with the initial velocity ratio, particularly close to the spinneret. Fiber radius in layer 2 is significantly influenced by the die exit radius ratio. The neck-in tendency of fiber radius is more with the increase of the radius ratio near the take-up region.

5 References

1. J.A. Dantzig and C.L. Tucker, *Modeling in Materials Processing*. Cambridge University Press, Cambridge, 2001

2. J. S. Lee, D. M. Shin, H. W. Jung, J. C. Hyun, Stability analysis of a three-layer film casting process, Korea-Australia Rheology Journal, 19, No. 1, 2007, 27-33
3. R.E. Christensen, Extrusion coating of polypropylene, *S.P.E.J.*,18 (1962) pp.751
4. J.C. Miller, Swelling behavior in extrusion, *S.P.E.Trans.*, 3 (1963) pp. 134
5. S. Kase and T. Matsuo, Studies on Melt Spinning I. Fundamental Equations on the Dynamics of Melt Spinning, *J. Polym. Sci. Part A.* **3**, 2541 (1965)
6. M. A. Matovich and J. R. A. Pearson, Spinning a Molten Thread Line: Steady State Isothermal Viscous Flows, *Ind. Eng. Chem. Fund.* **8**, 512 (1969a)
7. J. R. A. Pearson and M. A. Matovich, Spinning a Molten Thread Line: Stability, Ind. Eng. Chem. Fund. **8**, 605 (1969b)
8. H. Ishihara and S. Kase, Studies on Melt Spinning V. Draw Resonance as a Limit Cycle, *J. Appl. Polym. Sci.* **19**, 557 (1975)
9. G. J. Donnelly and C. B. Weinberger, Stability of Isothermal Fiber Spinning of a Newtonian Fluid, *Ind. Eng. Chem. Fund.* **14**, 334 (1975)
10. R. G. D'Andrea and C. B. Weinberger, Effects of Surface Tension and Gravity Forces in Determining The Stability of Isothermal Fiber Spinning, *AICHE J.* **22**, 923 (1976)
11. Y. T. Shah and J. R. A. Pearson, On the Stability of Non-isothermal Fiber Spinning – General Case, *Ind. Eng. Chem. Fund.* **11**, 150 (1972)
12. Park C-W. A study on bicomponent two-layer slot cast coextrusion. Polymer Engineering and Science 1991;31:197–203.
13. J.A. Dantzig and C.L. Tucker, *Modeling in Materials Processing*. Cambridge University Press, Cambridge, 2001
14. R.E. Christensen, Extrusion coating of polypropylene, *S.P.E.J.*,18 (1962) pp.751
15. J. Zhang, R. E. Khayat, W. Wang, Stability of high-speed two-layer film casting of Newtonian fluids, Int. J. Numer. Meth. Fluids, 2006, 52, 31-61
16. J. S. Lee, D. M. Shin, H. W. Jung, J. C. Hyun, Stability analysis of a three-layer film casting process, Korea-Australia Rheology Journal, 19, No. 1, 2007, 27-33
17. B. Suman, P. Tandon, Fluid flow stability analysis of multilayer fiber drawing, Chem. Engg. Sc., 65, 2010, 5537-5549.
18. Z. U. Ahmed*, M. A. Wakil **"**Effects of gravity and fluid properties on isothermal high speed two-layer filament jet flow" ICME 11-FL-27, (ICME2011) 18-20 December 2011, Dhaka, Bangladesh.
19. Cao F. M.E.Sc. Thesis, The University of Weastern Ontario, London, Ontario, Canada, 2003.